MOLECULAR AND CELLULAR BIOLOGY, Feb. 1997, p. 677–686 Vol. 17, No. 2
0270-7306/97/$04.00+0

The Intracisternal A-Particle Proximal Enhancer-Binding Protein Activates Transcription and Is Identical to the RNA- and DNA-Binding Protein p54^{nrb}/NonO

AMITABHA BASU,[1] BENHAO DONG,[2]† ADRIAN R. KRAINER,[2] AND CHIN C. HOWE[1]*

The Wistar Institute, Philadelphia, Pennsylvania 19104,[1] and Cold Spring Harbor Laboratory, Cold Spring Harbor, New York 11724-2208[2]

Received 26 July 1996/Returned for modification 26 September 1996/Accepted 11 November 1996

The long terminal repeats of murine intracisternal A particles (IAPs) contain an IAP proximal enhancer (IPE) element that is inactive in murine F9 embryonal carcinoma cells and active in the parietal endoderm cell line PYS-2. The element binds efficiently to a 60-kDa IPE-binding protein (IPEB) present in PYS-2 cells but poorly to F9 proteins, suggesting a role for IPEB in regulating IAP expression. We have purified calf thymus IPEB, which binds to the IPE and transactivates a reporter gene in HeLa cell extracts. Based on the peptide sequence of the purified calf IPEB, we have cloned a 420-bp cDNA and showed that the encoded protein is the homolog of human p54^{nrb} and mouse NonO, which are characterized by the presence of two RNA recognition motifs. We show that p54^{nrb} is an IPE-binding transcription activator with its DNA-binding and activation domains in the N- and C-terminal halves, respectively. The activation domain of p54^{nrb} is active in HeLa, PYS-2, and F9 cells, whereas p54^{nrb} as a whole molecule is active in HeLa and PYS-2 cells but not in F9 cells. Thus, the lack of activity of p54^{nrb} in F9 cells is due to an ineffective DNA-binding domain. We demonstrate that p54^{nrb} also binds to a pre-mRNA. Based on the close sequence relatedness of this protein to PSF, which is required for pre-mRNA splicing in vitro, we discuss the possibility that p54^{nrb} has dual roles in transcription and splicing.

Murine intracisternal A particles (IAPs) are defective endogenous retroviruses encoded by proviral elements that are reiterated 2,000 times and dispersed throughout the genome. IAPs are constitutively expressed at high levels in many mouse tumors and at basal levels in most normal adult mouse tissues (reviewed in references 21 and 22). In tumor cells where IAPs are actively expressed, these elements transpose and act as insertional mutagens via integration of actively synthesizing extrachromosomal viral DNA to new sites in the host genome. Such transpositions induce aberrant expression of target genes, contributing to augmented growth autonomy of the host cell and thus to the process of neoplastic transformation (21, 22, 25). Several germ line insertions contributing to mutagenesis have also been found (7, 22). Thus, investigation of the mechanism of IAP transcriptional activation should ultimately lead to an understanding of the role of endogenous retroviruses in transposition-induced mutagenesis.

IAP proviral elements contain in their long terminal repeats (LTRs) all of the *cis*-acting elements required for the enhancement of IAP gene transcription (8, 23, 26). The *cis* elements and their interacting transcription factors identified so far include the Enh1 and Enh2 elements located between nucleotides (nt) −164 and −110, which bind to EBP-80 of murine myeloma cells (13, 14), and sites located at the 5′ end of the LTR between nt −210 and −168, which bind to 28- and 46-kDa proteins of murine PCC3 embryonal carcinoma (EC) cells (40). In our analyses of the mechanism by which IAP expression becomes activated, we have found that IAP gene expression in murine F9 EC cells, which resemble early embryonic cells, is restricted, whereas upon differentiation of these cells into parietal endoderm-like cells, IAP expression becomes highly activated. IAP expression is also activated in the parietal endoderm cell line PYS-2 (18). Two DNA elements have been identified. An IAP upstream enhancer element located between nt −186 and −167 is active in both F9 and PYS-2 cells and binds to the 65-kDa zinc finger protein YY1 in a CpG methylation-dependent manner, suggesting that IAP expression is regulated by site-specific methylation (32). We also identified an IAP proximal enhancer (IPE) element that is inactive in F9 cells and active in PYS-2 cells; the IPE binds efficiently to a 60-kDa protein expressed in PYS-2 cells but inefficiently to the corresponding protein in F9 cells (24). The 60-kDa IPE-binding protein (IPEB) is expressed in adult thymocytes and activated splenic B cells (19), corresponding to the pattern of IAP expression (27). These results suggest that the IPE element and the 60-kDa IPEB play a role in regulating the expression of the IAP gene.

In this present study, we have purified the 60-kDa IPEB from calf thymus, cloned a cDNA fragment thereof, and shown that this protein is the homolog of human p54^{nrb} and mouse NonO (10, 38). NonO is a recently isolated DNA-binding protein that recognizes an octamer motif in the immunoglobulin heavy-chain promoter. NonO contains two RNA recognition motifs (RRMs), each with two ribonucleoprotein (RNP) consensus sequences (RNP1 and RNP2) known to bind to RNA and single-stranded DNA (3, 4, 9, 33, 38). The NonO RRMs bind to the single-stranded octamer motif, while a domain that binds with low affinity to the double-stranded octamer motif lies immediately downstream from the RRMs. Using cloned p54^{nrb}, we show that, like calf thymus and endogenous PYS-2 IPEB, p54^{nrb} binds to the IPE, which has little similarity to the octamer motif, and activates transcription from target genes. We also demonstrate that p54^{nrb} is a pre-mRNA-binding protein.

* Corresponding author. Mailing address: The Wistar Institute, 3601 Spruce St., Philadelphia, PA 19104. Phone: (215) 898-3796. Fax: (215) 898-3868.

† Present address: New York University Medical Center, New York, N.Y.

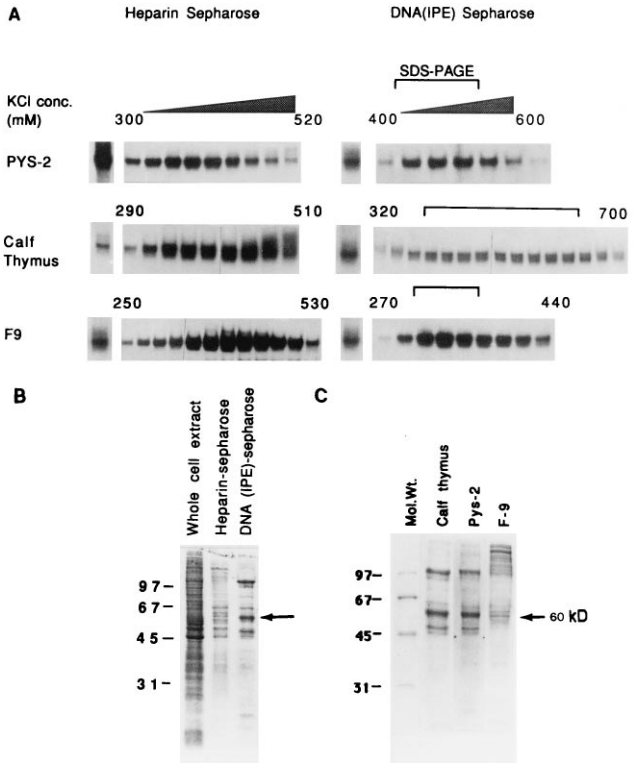

FIG. 1. Partial purification of IPEB from F9 cells, PYS-2 cells, and calf thymus. (A) Band shift assays. Equal amounts of total protein from whole-cell extracts from calf thymus, PYS-2, and F9 cells were fractionated twice on an HS column and twice on a DNA affinity column. Band shift assays were performed with each chromatographic fraction, using the IPE sequence as a probe. To identify the electrophoretic migration of the IPEB-IPE complex, PYS-2 nuclear extracts were also used to bind to the IPE sequence (first lane from the left of each panel). Results from the second chromatographic cycle are shown. Fractions pooled for SDS-PAGE analysis shown in panel C are indicated. The concentrations of KCl necessary to elute IPE-binding activity are indicated. (B) SDS-PAGE of the calf thymus extract at different stages of purification. Thirty-microgram aliquots of proteins in the eluates of the second cycle of HS and DNA affinity chromatography were electrophoresed and visualized by Coomassie blue staining. The arrow indicates the major 60-kDa protein. (C) SDS-PAGE of 30 μg of twice-affinity-purified proteins from calf thymus, PYS-2, and F9 extracts. Molecular masses are indicated in kilodaltons.

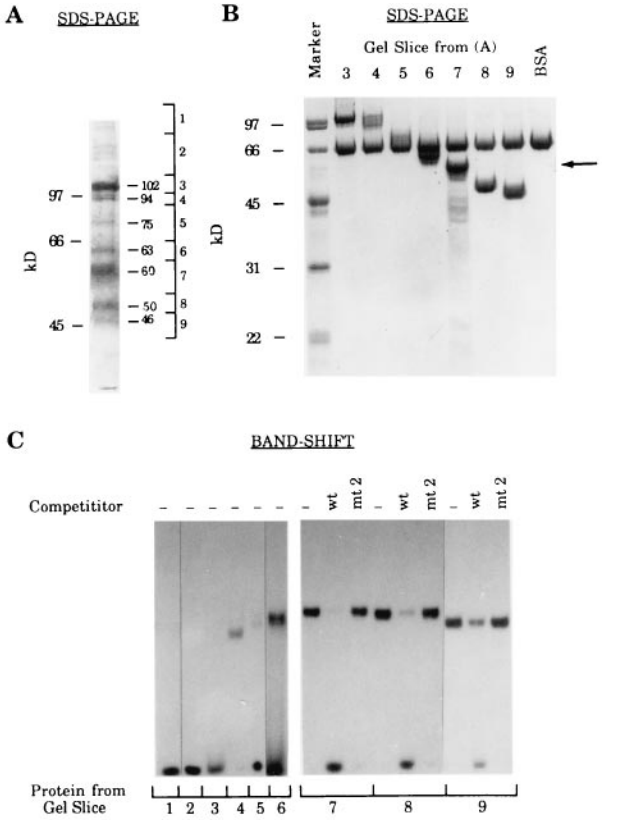

FIG. 2. Purification of IPEB by preparative SDS-PAGE. (A) SDS-PAGE of DNA affinity-purified calf thymus IPEB. Proteins (150 μg) in the second-cycle DNA column eluate were electrophoresed, and an end strip was cut from the preparative gel and stained with Coomassie blue for visualization. The 60-kDa IPEB and proteins of other sizes were isolated from the gel. (B) Analysis of 10 μg each of the isolated proteins. The arrow indicates the band representing BSA, used to facilitate efficient precipitation and isolation of IPEB. (C) Band shift analysis of the isolated proteins. About 50-ng aliquots of isolated proteins were incubated without or with a 100-fold excess of the indicated competitors and allowed to bind to ^{32}P-labeled IPE. wt, the wild-type unlabeled IPE; mt 2, the IPE mt2 oligonucleotide (see Materials and Methods for sequences).

MATERIALS AND METHODS

Synthetic oligonucleotides. The sequences of oligonucleotides spanning nt −59 to −39 (IPE) of the IAP LTR (22) and containing the IPEB-binding site (GAGTGAC) and mutations (mt2 to mt4) within the binding site are as follows: IPE, GATCATCAGGGAGTGACACGTCCGA; IPE mt2, GATCATCAGGGAATTTACGTCCGA; IPE mt3, GATCATCAGTTTGTGACACGTCCGA; IPE mt4, GATCATCAGGGAGTGTTGCGTCCGA; and CRE, GATCTTCCCCGTGACGTCAACTCGGC. Mutated nucleotides are underlined. The CRE oligonucleotide spanning nt −96 to −75 of the IAP LTR (23) contains the IPEB recognition sequence (GTGAC). Only coding strands are shown.

Cell culture, preparation of nuclear and whole-cell extracts, and purification of IPEB. Murine F9 and PYS-2 cell cultures and their nuclear and whole-cell extracts, and whole-cell extracts from calf thymus, were prepared as described previously (19). Purification of IPEB by sequence-specific DNA affinity chromatography has been described elsewhere (19). Calf thymus proteins obtained after two cycles of heparin-Sepharose (HS) column chromatography and two cycles of DNA affinity chromatography were purified on preparative sodium dodecyl sulfate (SDS)-polyacrylamide gels as described previously (16), with modifications. Briefly, proteins in the column eluate were resolved by SDS–10% polyacrylamide

TABLE 1. Purification of IPEB

Source	Fraction	Total protein (mg)	Total activity[a] (U)	Sp act (U/mg)	Purification (fold)	Yield (U)
PYS-2	Whole-cell extract	90	8,182	91		100
	HS 2nd cycle	44	5,714	130	1.4	70
	DNA affinity 2nd cycle	0.32	3,200	10,000	110	39
Calf thymus	Whole-cell extract	4,200	232,044	55		100
	HS 2nd cycle	306	102,000	333	6.1	44
	DNA affinity 2nd cycle	6	54,545	9,090	165	24
	SDS-PAGE (P60)	0.4	40,000	100,000	1,818	17

[a] One unit of activity is the amount of protein required to shift 1 fmol of probe out of 10 fmol in the presence of 1 μg of poly(dI-dC).

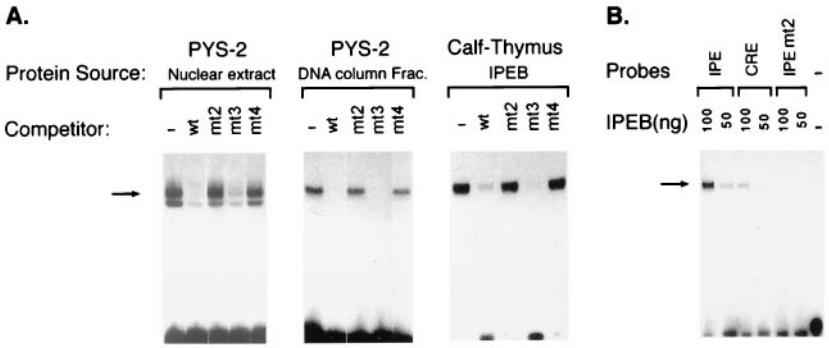

FIG. 3. DNA-binding specificity of the purified 60-kDa calf thymus IPEB. (A) Competition experiments. The SDS-PAGE-purified calf thymus IPEB and, as controls, the partially purified PYS-2 IPEB after the second cycle of the DNA affinity chromatography and the unpurified IPEB in PYS-2 nuclear extracts were incubated without or with a 100-fold excess of the indicated competitors and then with the IPE probe. The resulting complexes were analyzed by band shift assays. wt, the wild-type unlabeled IPE sequence; mt2, mt3, and mt4, IPE mutant oligonucleotides (see Materials and Methods for sequences). (B) Band shift assays with the CRE sequence. The purified calf thymus IPEB was incubated with probe IPE, CRE, or IPE mt2, and the complexes were analyzed. The amounts of IPEB used in the binding reactions are indicated above the lanes. The arrow shows the migration position of the IPEB-IPE complex.

gel electrophoresis (PAGE). A strip was cut from the gel, stained with Coomassie blue, and used as a guide to isolate proteins in various regions of the gel. Proteins were then precipitated at −20°C with acetone in the presence of 0.1 mg of bovine serum albumin (BSA; molecular biology grade; Boehringer Mannheim) per ml. The precipitate was resuspended in 6 M guanidine to denature the protein and then renatured by dialysis into band shift binding buffer containing 25 mM HEPES (pH 7.9), 60 mM KCl, and 5% glycerol.

Band shift assays and in vitro transcription. Band shift assays were carried out as described previously (19). For in vitro transcription, template DNA was prepared by *Pvu*II digestion to generate runoff transcripts of 300 nt. Transcription reactions were carried out in a volume of 25 μl containing 0.1 μg of template DNA, 60 to 80 μg of nuclear extract, 10 μCi of [α-^{32}P]UTP (3,000 Ci/mmol; Amersham), 0.4 mM each ATP, CTP, and GTP, and 33 μg of poly(dI-dC) per ml at 30°C for 60 min in buffer containing 20 mM HEPES (pH 7.9), 100 mM KCl, 3 mM $MgCl_2$, 0.2 mM EDTA, 0.5 mM dithiothreitol (DTT), and 20% glycerol. Runoff transcripts were analyzed on a denaturing 6% polyacrylamide sequencing gel.

Tryptic digestion of purified IPEBs, peptide sequencing, and RT-PCR. DNA affinity column-purified calf thymus proteins were fractionated by SDS-PAGE, transferred onto a polyvinylidene difluoride membrane (Bio-Rad), and visualized by Coomassie blue staining. Proteins of 63, 60, 50, and 45 kDa were excised and digested in situ with trypsin (1), and the resulting peptides were separated by reverse-phase high-performance liquid chromatography (HPLC). Peptide sequencing (the Wistar Protein Microchemistry Facility) revealed six peptide sequences: NLEKQNHTPR, TFTQR, VELDNMPLR, CSEGSFLLTTFPR, FAQPGSFEYEYAMR, and WK (sequences a to e). Peptides c and e were used to synthesize degenerate primers. Since the relative order of the two tryptic fragments within IPEB was not known, a combination of sense and antisense degenerate oligonucleotides was used for reverse transcriptase-mediated PCR (RT-PCR) using calf thymus total RNA as the template. Four prominent amplified fragments were detected from the primer pair containing the sense peptide c and antisense peptide e. Hybridization with a probe containing the sequence 5′ to the antisense peptide e primer identified a 420-bp fragment as the correct RT-PCR product. This product was subcloned into pUC19 and sequenced.

Antibody production. Recombinant p54^{nrb} was expressed in *Escherichia coli* as described previously (10). Bacteria were resuspended and lysed by sonication in 20 mM HEPES-KOH (pH 8)–0.2 mM EDTA–20% glycerol–1 mM DTT–0.2 mM phenylmethylsulfonyl fluoride–6 M urea. The clarified extract was fractionated by Mono Q chromatography in the same buffer. The flowthrough was applied to a Mono S column, and bound material was eluted with a 0 to 1 M NaCl gradient in the same buffer. Fractions containing pure p54^{nrb} were pooled, and urea was removed gradually by dialysis. Purified protein was used to immunize BALB/c mice and to prepare monoclonal antibodies at the Cold Spring Harbor Monoclonal Antibody Facility. A single specific anti-p54^{nrb} immunoglobulin M (IgM) monoclonal antibody was obtained.

Western blot analysis. Proteins were separated by SDS-PAGE and electroblotted onto nitrocellulose membranes (Micron Separations, Inc.). Immunoblotting was performed as described previously (2), using a monoclonal antibody (IgM) to p54^{nrb} and goat anti-mouse immunoglobulins (IgG, IgM, and IgA) conjugated to alkaline phosphatase (Cappel) as the second antibody.

In vitro transcription and translation of p54^{nrb} and binding of the encoded protein to the IPE sequence. Full-length and N- and C-terminal halves of p54^{nrb} were subcloned into pBluescript (Stratagene) and transcribed with T3 polymerase (Promega). Subcloning of N and C termini was accomplished by PCR with primers that incorporated an in-frame termination codon and a Kozak sequence surrounding an in-frame ATG initiation codon, respectively. The resulting templates were transcribed and capped by using a kit (Stratagene) according to the manufacturer's specifications, and plasmid DNA was digested with RNase-free DNase (Boehringer Mannheim). The capped mRNA was then translated in vitro in a rabbit reticulocyte lysate (Promega) in the presence or absence of [^{35}S]methionine. As a control, a luciferase cDNA in pBluescript was transcribed and translated. The translated nonradioactive products were used in band shift as-

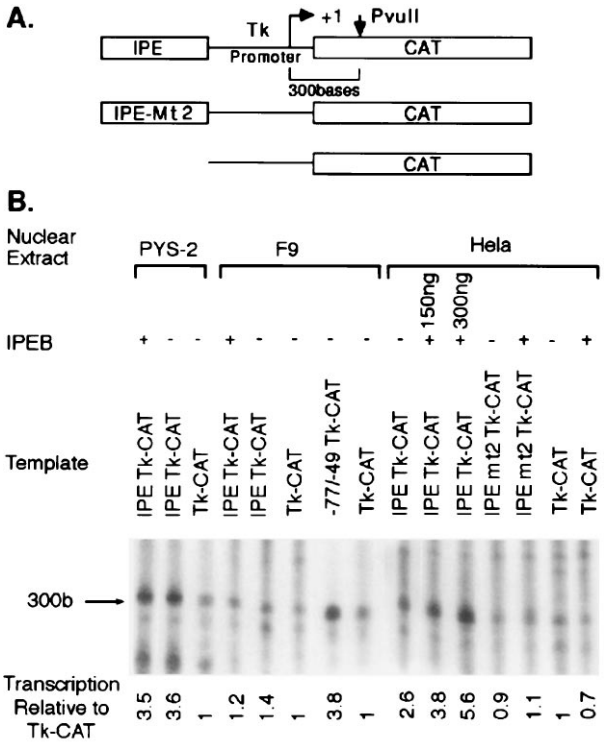

FIG. 4. IPEB stimulates in vitro transcription from an IPE promoter. (A) Templates for in vitro transcription reactions. IPE TK-CAT and IPE mt2 TK-CAT contain five copies of wild-type and mutated IPEB binding site, respectively, inserted in front of a TK-CAT reporter. *Pvu*II sites were used to linearize the templates, and the expected runoff transcript is 300 bases. (B) In vitro transcription assays. Template DNA (100 ng) was transcribed in vitro in PYS-2, F9, or HeLa extracts in the presence (+) or absence (−) of 300 ng of purified 60-kDa calf thymus IPEB unless indicated otherwise. −77/−49 TK-CAT contains three copies of a sequence located between nt −77 and −49 in the IAP LTR (21).

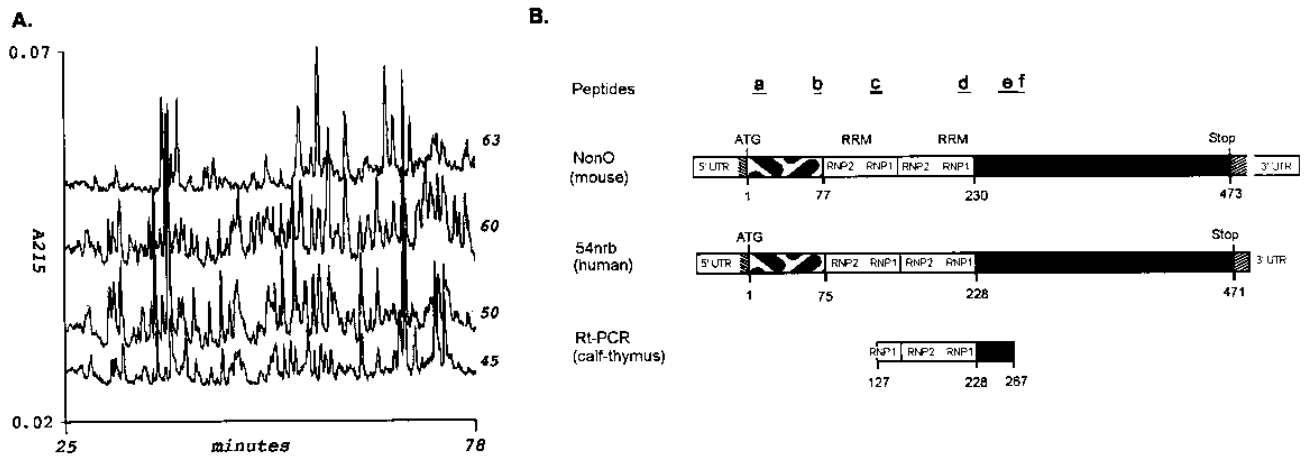

FIG. 5. Identification of calf thymus IPEB. (A) Reverse-phase HPLC of tryptic peptides from the SDS-PAGE-purified 63-, 60-, 50-, and 46-kDa calf thymus proteins. Absorbance profiles within retention times of 25 to 78 min are shown. The full scale of each chromatogram corresponds to 0.05 (0.02 to 0.07) absorbance unit at 215 nm. (B) Schematic comparison of murine NonO, human p54^{nrb}, and the RT-PCR product amplified from calf thymus RNA. RNP1 and RNP2, RNP consensus sequences; UTR, untranslated region. The locations of peptide sequences a to f (see Materials and Methods) identified in the SDS-PAGE-purified calf thymus IPEB are shown above the NonO sequence. Numbers below NonO and p54^{nrb} sequences represent amino acid positions of the respective proteins (10, 38). Numbers in the RT-PCR product from calf thymus are based on the p54^{nrb} sequence.

says. The radioactive proteins were bound to a DNA affinity column as described previously (19). The bound proteins, and as a control the unpurified total translated products, were precipitated with acetone in the presence of BSA, separated by SDS-PAGE, and visualized by autoradiography.

Systematic evolution of ligands by exponential enrichment (SELEX). An RNA library of 68-mers containing a central 25-nt degenerate region was prepared as previously described (36). Five nanomoles of initial RNA pool was incubated with 50 pmol of purified recombinant p54^{nrb} at 30°C for 30 min in 200 μl of buffer containing 20 mM HEPES (pH 7.3), 3.2 mM $MgCl_2$, 60 mM KCl, and 0.5 mM DTT and filtered through a nitrocellulose disc prewetted with the same buffer. The disc was washed twice in the same buffer and extracted with a mixture containing 400 μl of phenol (pH 6.3) and 200 μl of 7 M urea in an Eppendorf tube with agitation for 30 min at room temperature. After addition of 200 μl of H_2O and vortexing, the sample was centrifuged for 10 min at 4°C, and RNA was recovered from the aqueous phase by ethanol precipitation. Further steps of amplification and selection (total of five rounds) and final subcloning and sequencing were performed as described previously (36).

UV cross-linking. Human β-globin pre-mRNA or mRNA comprising the first exon and most of the second exon (with or without the first intron) was prepared by in vitro transcription with SP6 RNA polymerase, using *Bam*HI-linearized plasmids SP64-HβΔ6 and SP64-HβΔ6-IVS1,2 (20) in the presence of [α-^{32}P]ATP, -GTP, -CTP, and -UTP. Twenty femtomoles of uniformly labeled RNA was incubated with 0, 3, 9, or 27 pmol of purified recombinant p54^{nrb} expressed in *E. coli*, in 15 μl of splicing buffer (20 mM HEPES-NaOH [pH 8], 100 mM KCl, 5% glycerol, 0.2 mM EDTA, 0.5 mM DTT) containing 50 ng of RNase-free BSA per ml, for 20 min at 30°C. The mixture was UV irradiated twice at 900 mJ/cm^2 in a Spectrolinker XL-100 UV crosslinker (Spectronics Co.), treated with 1.6 μg of RNase A at 37°C for 20 min, boiled for 3 min in SDS sample buffer, and loaded on an SDS–12% polyacrylamide gel. The gel was stained with Coomassie blue to locate the markers, dried, and analyzed by autoradiography.

Transfection assays. Cells were cotransfected with 4 μg of reporter plasmid, 3 μg of expression plasmid, and 5 μg of pRSV-LacZ (as an internal control for transfection efficiency) by the calcium phosphate precipitation method as described previously (32). The total amount of transfected DNA was adjusted to 12 μg with pUC18. The reporter plasmids, TK-CAT (pBLCAT2), $(GAL4)_5$-TK-CAT, and PYF TK-CAT, have been described elsewhere (32). IPE TK-CAT and IPE mt2 TK-CAT contain five copies of IPE and IPE mt2 inserted in front of TK-CAT, respectively. The expression plasmid pSV2-p54^{nrb} contains a full-length p54^{nrb} cDNA subcloned in the expression vector pECE, which contains the simian virus 40 early promoter and enhancer (11). pSV2GAL4(1-147) is the previously described pSG424 (32). pSV2GAL4(1-147)/N-term, pSV2GAL4(1-147)/C-term, and pSV2GAL4(1-147)/reverse C-term contain the N terminus, C terminus, or antisense C terminus of p54^{nrb}, respectively, inserted in frame in pSG424. Chloramphenicol acetyltransferase (CAT) assays were performed as described previously (23).

RESULTS

Purification of IPEB from calf thymus. We showed previously that among the mouse tissues examined, IPEB activity is most abundant in thymus and that this activity is conserved in various species, including calf (19). Thus, whole-cell extracts from calf thymus were used to obtain a large quantity of IPEB through two cycles of HS and two cycles of DNA affinity column chromatography. As controls, PYS-2 and F9 cell extracts were also fractionated. The IPE-binding activity of each chromatographic fraction was monitored by band shift assays. The IPE-binding activity in calf thymus extracts and in control PYS-2 and F9 extracts eluted between 0.25 and 0.55 M KCl in the first (not shown) and second cycles of HS chromatography, with respective peak fractions at 0.39, 0.4, and 0.41 M KCl (Fig. 1A). In a DNA affinity column, calf IPEB eluted between 0.32

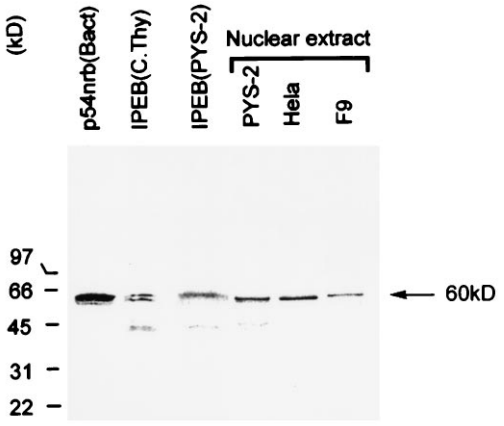

FIG. 6. Western blot analysis. p54^{nrb} synthesized in bacteria (Bact), SDS-PAGE-purified calf IPEB (C. Thy), twice-DNA-affinity-purified PYS-2 IPEB (PYS-2), and nuclear extracts from PYS-2, HeLa, and F9 cells were fractionated on an SDS–10% polyacrylamide gel and transferred to nitrocellulose for Western blotting. The filters were probed with a monoclonal antibody raised against human p54^{nrb} expressed in *E. coli*.

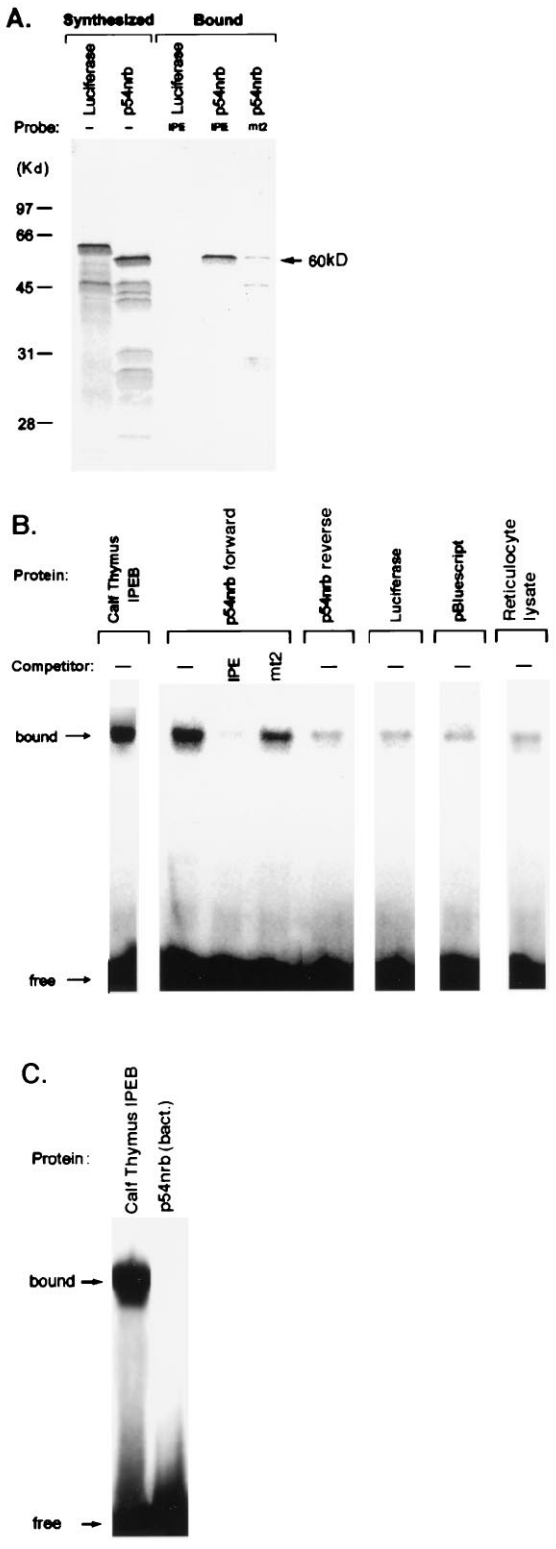

FIG. 7. Binding of p54^{nrb} to IPE. (A) DNA affinity chromatography. p54^{nrb} and control luciferase template DNAs were transcribed and translated in vitro and bound to resin containing either the IPE or IPE mt2 oligonucleotide in the presence of poly(dI-dC). The resin was washed, and bound protein was eluted with 1 M KCl and analyzed by SDS-PAGE. A 60-kDa protein encoded by p54^{nrb} bound efficiently to the IPE but not the IPE mt2 oligonucleotide. (B) Band shift assays with in vitro-translated p54^{nrb}. p54^{nrb} transcribed and translated in vitro in the forward (sense) orientation was incubated with the IPE probe in the presence or absence of a 50-fold excess of the indicated competitors. As controls, proteins were transcribed and translated from p54^{nrb} cDNA in the reverse (antisense) orientation, luciferase cDNA, or pBluescript vector or in the absence of template DNA (reticulocyte lysate alone). The faint bands in the control lanes represent complexes derived from the endogenous p54^{nrb} present in reticulocyte lysates. (C) Band shift assay with recombinant p54^{nrb}. p54^{nrb} synthesized in bacteria (bact.) was incubated with the IPE probe. No complex comigrating with the IPE-calf thymus IPEB complex is visible.

to 0.7 M KCl, with the peak fraction at 0.52 M KCl, while PYS-2 IPEB eluted between 0.4 and 0.6 M KCl, peaking at 0.49 M, and F9 IPEB eluted between 0.27 and 0.44 M KCl, with a peak fraction at 0.35 M. The fact that calf IPEB and PYS-2 IPEB elution peaked around similar salt concentrations (0.52 and 0.49 M, respectively), while F9 IPEB elution peaked at a much lower salt concentration (around 0.35 M KCl), suggests that DNA-binding affinities of calf thymus and PYS-2 IPEB are similar and both differ from that of F9 IPEB. Table 1 summarizes the purification of IPEB. Major purification occurred with the DNA affinity chromatography, resulting in 110- and 165-fold enrichment over levels for the initial PYS-2 and calf thymus extracts, respectively. SDS-PAGE analysis of IPEB-containing calf thymus fractions at each step of purification further revealed that a 60-kDa protein was enriched as the most prominent protein in the DNA affinity eluate (Fig. 1B). Consistent with previous findings (23), SDS-PAGE analysis of equal amounts of twice-affinity-purified proteins also revealed that the 60-kDa IPEB-binding activity is abundant in PYS-2 but not in F9 cells (Fig. 1C).

The affinity-purified calf thymus proteins were further purified by preparative SDS-PAGE (Fig. 2A). Individual proteins were isolated from the gel and reanalyzed by SDS-PAGE (Fig. 2B). Band shift analysis of the renatured proteins (Fig. 2C) showed that the 60-kDa protein and the less abundant 63-, 50-, and 45-kDa proteins independently bound to the IPE sequence. Among these proteins, binding of the 63-kDa species was the weakest. Competitive binding experiments indicated that the unlabeled IPE sequence competed efficiently with the labeled IPE probe for binding to the 60-kDa protein but less efficiently with the probe for binding to the 50- and 45-kDa proteins. The mt2 oligonucleotide, which contains a mutation within the IPE sequence, failed to compete for binding to all three proteins. Thus, the 60-kDa calf thymus protein contains the IPEB activity. Hereafter, the 60-kDa calf thymus protein is referred to as the calf thymus IPEB. The significance of the 50- and 45-kDa proteins will be discussed below.

The DNA-binding specificity of the purified calf thymus IPEB was then compared to that of endogenous PYS-2 IPEB in nuclear extracts. In band shift assays, the purified calf thymus IPEB and the DNA affinity-purified PYS-2 IPEB bound to the IPE probe and yielded complexes with electrophoretic mobilities identical to that of the complex produced from the binding of the unfractionated PYS-2 IPEB in nuclear extracts to the IPE probe (Fig. 3A). The three complexes showed identical competition patterns with unlabeled IPE oligonucleotide and with mutant oligonucleotides. The unlabeled IPE sequence competed efficiently with the probe for IPEB binding. IPE mt2, which contains a 5-bp mutation within the IPE element, and IPE mt4, which has a 3-bp mutation toward the 3′ end of the binding site, failed to compete for IPEB binding. IPE mt3, which has a 3-bp mutation toward the 5′ end of the binding site, competed efficiently for IPEB binding. The results further support the conclusion that the 60-kDa calf thymus protein is an IPEB and that the major recognition site is GTGAC located between nt −51 to −47, refined from GAGTGAC identified previously by methylation interference assays (24).

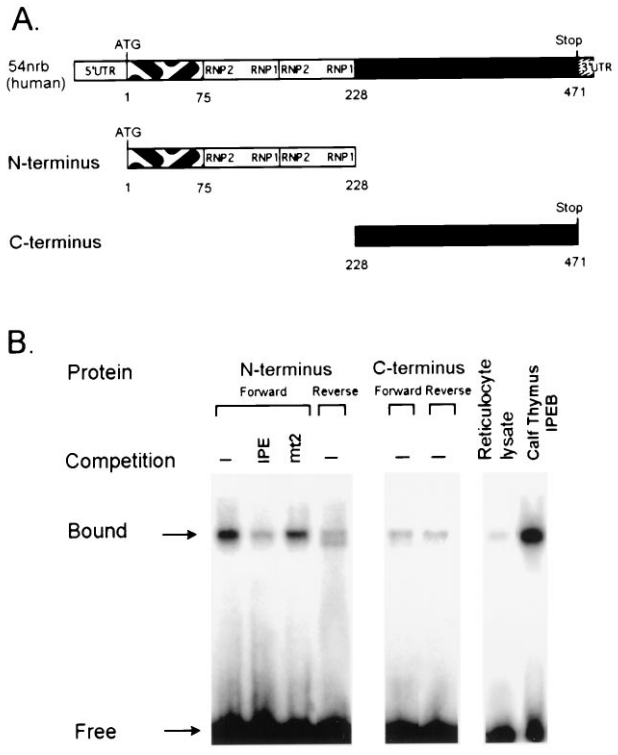

FIG. 8. Characterization of the DNA-binding domain of p54^{nrb}. (A) Schematic representation of N- and C-terminal p54^{nrb} translated from reticulocyte lysates. Abbreviations are as in Fig. 5B. (B) Band shift analysis. N and C termini of p54^{nrb} synthesized with reticulocyte lysates in the forward (sense) and reverse (antisense) orientations were incubated with the IPE probe in the presence or absence of a 50-fold excess of competitors, the IPE and IPE mt2 oligonucleotides. As controls, reticulocyte lysate and calf thymus IPEB were also used in band shift assays.

Since the CRE oligonucleotide contains the IPEB-binding-site sequence GTGAC (see Materials and Methods for the sequence), the ability of the calf thymus IPEB to bind to the CRE oligonucleotide was tested (Fig. 3B). Band shift assays indicated poor binding of the protein to the CRE, while the same amount of IPEB was able to bind the IPE sequence and to form a IPEB-IPE complex in a sequence-specific manner, being unable to bind to the IPE mt2 sequence. Thus, in addition to the binding site sequence, the flanking sequence influences IPEB-binding activity. This conclusion is consistent with our observation that a PYS-2 nuclear protein-IPE sequence complex migrates differently than a CRE sequence complex of the same nuclear protein (our unpublished results).

Transcriptional activity of the purified 60-kDa IPEB. To further confirm the identity of the purified calf IPEB, we analyzed the transcriptional potential of the protein. In vitro runoff transcription experiments were performed with nuclear extracts derived from F9, PYS-2, and HeLa cells and, as a template, an IPE TK-CAT reporter plasmid containing five copies of the oligonucleotide encompassing the IPE (Fig. 4). In the absence of exogenous IPEB, the endogenous IPEB in the HeLa extract directed transcription from the IPE TK-CAT plasmid at 2.6 times the activity of TK-CAT. Addition of purified IPEB to the in vitro transcription mixture resulted in an additional increase in transcription in a dose-dependent manner, 1.5-fold at 150 ng and 2.2-fold at 300 ng. This transcriptional activation by endogenous or endogenous plus exogenous IPEB was abolished when the IPE was mutated (IPE mt2). Thus, purified IPEB acts as a sequence-specific transcriptional activator. The transcription by HeLa extracts was sensitive to α-amanitin (1 μg/ml) (not shown), indicating that transcription is mediated by RNA polymerase II.

As expected from previous studies (24), the endogenous IPEB in PYS-2 extracts led to efficient transcription of the IPE TK-CAT reporter gene (Fig. 4). Addition of purified IPEB did not result in any measurable increase in transcription, possibly due to the abundance of the endogenous factor. The F9 extract, on the other hand, failed to give a measurable increase in transcription from the IPE TK-CAT plasmid above the level obtained with TK-CAT, either in the presence or in the absence of exogenous IPEB. The possibility that such failure was due to poor extract preparations was ruled out since the F9 extract was shown to direct active transcription from a plasmid containing a different DNA element located between nt −77 and −49 of the IAP LTR (Fig. 4). In a mixing experiment, addition of F9 extracts to PYS-2 extracts abolished the ability of the latter to activate transcription, suggesting that the putative F9 inhibitor is dominant (results not shown).

Tryptic maps of 63-, 60-, 50-, and 45-kDa IPEBs. The relationship between the 60-kDa IPEB and other IPEBs was investigated by tryptic mapping (Fig. 5A). The 60-, 50-, and 45-kDa proteins, which bind efficiently to the IPE sequence, gave nearly identical tryptic maps, whereas the 63-kDa protein, which binds weakly to the IPE sequence, gave a different profile. Thus, the 60-, 50-, and 45-kDa proteins are closely related, while the 63-kDa protein is likely an unrelated protein. Among six peptide sequences (a to f; Fig. 5B) isolated from the 60-kDa protein and analyzed, sequence a is present in the 45-kDa protein while sequence d is present in the 50-kDa protein, indicating that the three proteins may represent posttranslationally modified or differentially spliced products or proteolytic products.

Identification of IPEB as NonO/p54^{nrb}. Two peptide sequences (c and C-terminal half of e; Fig. 5B) from the 60-kDa calf thymus IPEB were used to prepare degenerate oligonucleotide primers for RT-PCR using calf thymus RNA as the template. A 420-bp amplified cDNA gave positive hybridization to a probe containing a nucleotide sequence corresponding to the N-terminal half of peptide e; this cDNA was subcloned into pUC19 and sequenced. Searches of DNA databases revealed that the amplified cDNA has complete sequence homology to NonO (97.2% at the nucleotide level and 97% at the amino acid level) cloned from BCL_1 cells (38) and to its human homolog p54^{nrb} (98.4% at the nucleotide level and 98.6% at the amino acid level) cloned from HeLa cells (10). Furthermore, all of the peptide sequences identified in the purified 60-kDa calf IPEB are present in NonO/p54^{nrb} (Fig. 5B). Thus, IPEB is very likely the homolog of NonO/p54^{nrb}.

A monoclonal antibody to p54^{nrb} recognizes IPEB. Western analysis (Fig. 6) showed that a monoclonal antibody to p54^{nrb} synthesized in bacteria reacted not only with the recombinant p54^{nrb} protein, as expected, but also with the SDS-PAGE-purified calf thymus IPEB and the DNA affinity-purified PYS-2 IPEB. All three proteins have an apparent molecular mass of 60 kDa. Analysis of nuclear extracts revealed the presence of antibody-reactive 60-kDa proteins not only in PYS-2 and HeLa cells, where the endogenous 60-kDa IPEB is functionally active as indicated by the in vitro transcription assays, but also in F9 extracts, where the 60-kDa IPEB is functionally inactive. Thus, IPEB is present in F9 cells.

p54^{nrb} is a sequence-specific DNA-binding protein that recognizes the IPE. The in vitro-transcribed and -translated p54^{nrb}, like the purified calf thymus IPEB, bound efficiently to DNA affinity resin containing the IPE but not to that contain-

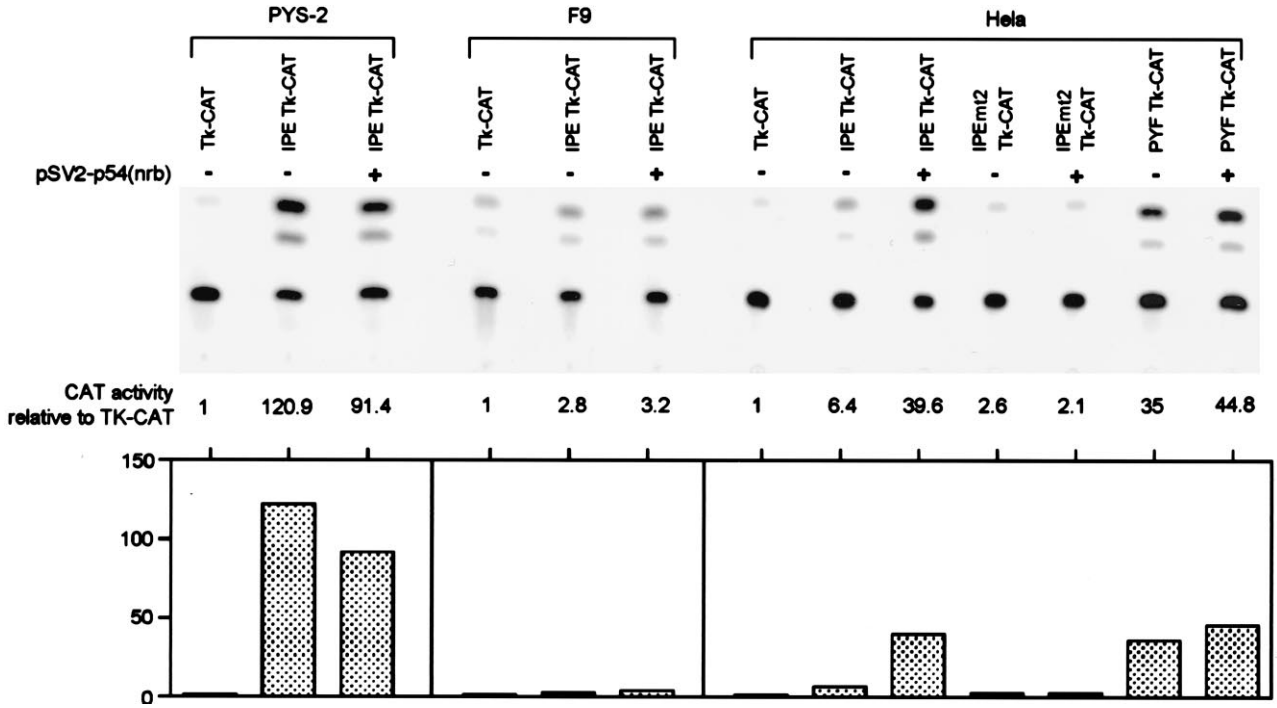

FIG. 9. Transcriptional activity of p54^{nrb} in vivo. PYS-2, F9, and HeLa cells were transfected with the reporter gene IPE TK-CAT and, as controls, with TK-CAT and IPE mt2 TK-CAT in the absence (−) or presence (+) of the p54^{nrb} expression plasmid, pSV2-p54^{nrb}. The upper panel shows the autoradiograms of products from CAT assays. The lower panel illustrates the CAT activity relative to TK-CAT activity, set at 1. Results are the averages of six independent transfections, and the standard deviation did not exceed 2.7. Cotransfection with empty expression vector pECE gave only basal activity (results not shown). PYF TK-CAT has been described elsewhere (21).

ing IPE mt2 (compare Fig. 7A with Fig. 3A). The control in vitro-translated luciferase did not bind to the DNA affinity column containing IPE. In band shift assays (Fig. 7B), p54^{nrb} synthesized in the forward (sense) orientation in reticulocyte lysate also bound to the IPE and produced a DNA-protein complex comigrating with the complex produced from the binding of the IPE to the purified calf thymus IPEB (Fig. 7B, lanes 1 and 2). Moreover, the two complexes, IPE-p54^{nrb} and IPE-calf thymus IPEB, showed identical competition patterns; the unlabeled IPE was an efficient competitor, while IPE mt2 was not (compare Fig. 7B with Fig. 3A). Thus, p54^{nrb} has the same binding specificity as the calf thymus IPEB. As controls, we also translated p54^{nrb} in reverse (antisense) orientation, luciferase, and proteins from empty vector pBluescript in reticulocyte lysates. The translated proteins from all of these controls formed a faint complex band comigrating with the IPE-p54^{nrb} complex (Fig. 7B; compare lanes 5 to 7 with lane 2). Incubation of the reticulocyte lysate with the IPE probe also yielded the same faint comigrating complex band (lane 8), suggesting the presence of endogenous p54^{nrb} or a related protein in the reticulocyte lysate. Thus, the faint complex bands produced in control lanes likely represent those derived from the endogenous p54^{nrb} present in the reticulocyte lysates. The protein synthesized in bacteria failed to bind to the IPE (Fig. 7C). This is unlikely to be the result of incorrect folding, since the same protein is capable of binding RNA (see below). The failure to bind DNA suggests that posttranslational modification is required for efficient DNA binding.

Localization of the DNA-binding domain of p54^{nrb}. The N-terminal half of p54^{nrb} comprises two canonical RRMs (10). The same region of the mouse homolog, NonO, binds to single-stranded DNA and RNA (36). We thus generated N- and C-terminal peptides by in vitro transcription of subclones containing appropriate domains of p54^{nrb} and used the translated peptides for band shift assays (Fig. 8B). The N-terminal peptide translated in the forward (sense) orientation bound to the IPE probe (lane 1). Interestingly, even though the N-terminal peptide is half the size of the full-length p54^{nrb} (calf thymus IPEB), the two complexes had essentially identical electrophoretic mobilities (compare lanes 1 and 8). The control N-terminal peptide translated in the reverse (antisense) orientation yielded a faint comigrating complex band (lane 4). The C-terminal peptide synthesized in the forward or reverse orientation or the reticulocyte lysate alone also produced a faint comigrating complex (lanes 5 to 7). Thus, as in Fig. 7B, the faint complex bands (Fig. 8B, lanes 2 and 4 to 7) likely represent complexes derived from the endogenous p54^{nrb} present in the reticulocyte lysate.

p54^{nrb} transactivates target genes in vivo. To further test the function of p54^{nrb} as an IPEB, we analyzed its ability to activate transcription from the IPE sequence by cotransfection assays (Fig. 9). Expression plasmid pSV2-p54^{nrb} was cotransfected with the reporter plasmid IPE TK-CAT into HeLa, PYS-2, and F9 cells. In HeLa cells, the endogenous IPEB itself mediated an approximately sixfold increase in CAT activity. Cotransfection of pSV2-p54^{nrb} resulted in an additional sixfold increase in the levels of CAT activity. The ability of p54^{nrb} expressed from pSV2-p54^{nrb} to activate transcription is IPE sequence specific, since mutation within the IPE abolished the ability of p54^{nrb} to stimulate CAT activity. The possibility that p54^{nrb}, being an RNA-binding protein, stabilizes the reporter mRNA and thus increases the steady-state CAT mRNA levels was ruled out, since the PYF TK-CAT reporter, which contains a mutant polyomavirus enhancer, failed to respond to cotransfected p54^{nrb}. In PYS-2 cells, the endogenous IPEB stimulated CAT activity 120-fold, and cotransfection with the expression plasmid resulted in a slight decrease in CAT activity, suggesting the presence of a titratable cellular factor that interacts with IPEB.

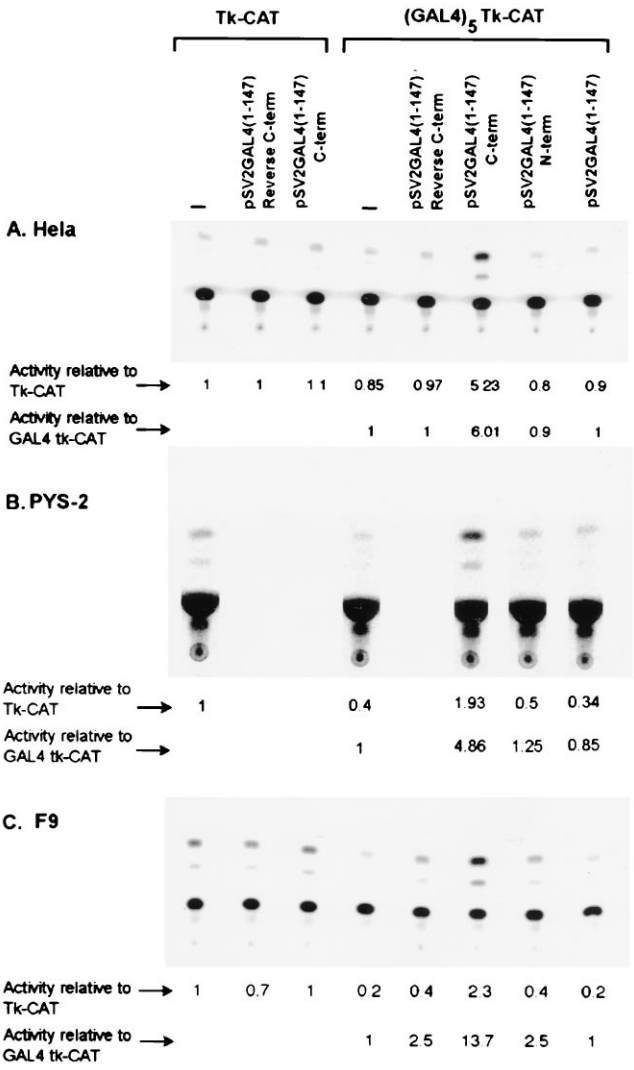

FIG. 10. Characterization of the transcriptional activation domain of p54^{nrb}. HeLa, PYS-2, and F9 cells were cotransfected with reporter genes and plasmids expressing fusion proteins containing GAL4(1-147) and the N or C terminus of p54^{nrb}, as indicated. The relative CAT activities were calculated against the basal reporter plasmid TK-CAT and then against the reporter plasmid $(GAL4)_5$-TK-CAT [containing five copies of GAL4(1-147)] to illustrate transcriptional enhancement by cotransfected expression plasmids.

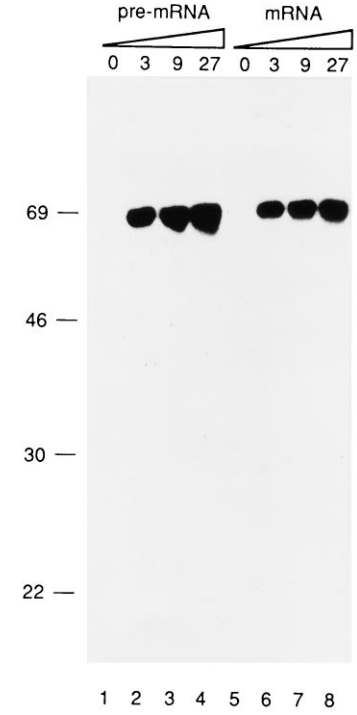

FIG. 11. p54^{nrb} binds RNA. Binding of purified, recombinant p54^{nrb} to β-globin RNA was assayed by UV cross-linking. Twenty femtomoles of in vitro-transcribed, uniformly labeled β-globin pre-mRNA or mRNA was incubated with the indicated amounts (picomoles) of recombinant p54^{nrb}, in buffer containing BSA, at 30°C for 20 min, UV irradiated, and digested with RNase A as described in Materials and Methods. The products were analyzed by SDS-PAGE and autoradiography. The positions of molecular weight markers are indicated in kilodaltons (note that the cross-linked RNA fragments result in slower mobility of p54^{nrb}).

The endogenous IPEB in F9 cells, on the other hand, did not stimulate any CAT activity, nor did cotransfection with the expression plasmid, suggesting that the transactivation activity of p54^{nrb} is inhibited in F9 cells.

To further confirm that p54^{nrb} is a transcription activator, the N-terminal (amino acids 1 to 228) and C-terminal (amino acids 228 to 471) halves of p54^{nrb} were expressed as fusion proteins with the GAL4 DNA-binding domain [GAL4(1-147)]. The plasmids expressing the fusion proteins were cotransfected with a TK-CAT reporter plasmid containing a GAL4 DNA-binding site into HeLa, PYS-2, and F9 cells (Fig. 10). In all three cell types, the C-terminus fusion protein enhanced transcription but the N-terminus fusion protein did not. Control experiments showed that the C-terminus activity was not due to the effect of the GAL4 DNA-binding domain, since the empty vector pSV2 GAL4(1-147) or the antisense C-terminus plasmid pSV2 GAL4(1-147)/reverse C-term produced only a basal level of reporter gene expression. Since the C-terminus fusion protein was an effective transactivator in F9 cells, whereas the full length protein was not (Fig. 9), we conclude that the DNA-binding domain, but not the activation domain, is defective in F9 cells.

p54^{nrb} is an RNA-binding protein. To determine if recombinant p54^{nrb} can bind RNA, the purified protein was incubated with radiolabeled pre-mRNA of 497 or 367 nt containing the first two exons of human β-globin with or without the first intron. Exposure to UV light resulted in cross-linking of p54^{nrb} to both RNAs, as determined by RNase A treatment followed by SDS-PAGE and autoradiography (Fig. 11). To determine if p54^{nrb} binds to a specific RNA sequence, a SELEX experiment was performed (Fig. 12). After five rounds of selection, p54^{nrb} preferentially bound short RNAs that were G rich and contained one or more copies of the consensus element AGGGA/U. We verified in filter binding experiments that the purified recombinant p54^{nrb} bound with higher affinity to short RNAs containing the SELEX motif than to control short RNAs lacking the motif, including a β-globin intron fragment (data not shown). Thus, the observed binding of p54^{nrb} to the β-globin RNAs that lack the SELEX motif (Fig. 11) is likely to be characterized by low affinity as well.

DISCUSSION

We showed previously that the transcriptional activity of a 60-kDa IPEB and its recognition motif IPE in the IAP LTR is high in PYS-2 cells but very low in F9 cells, suggesting that IPEB activity plays a role in active versus restricted expression of IAP in the corresponding cells (24). In the present study, we

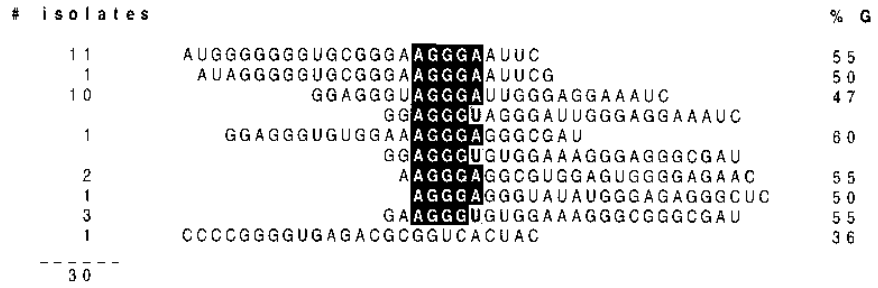

FIG. 12. Alignment of RNA sequences selected by p54^{nrb}. Five rounds of SELEX were carried out with an RNA library of 68-mers with 25 nt of degeneracy in the center and purified recombinant p54^{nrb}. RNA-protein complexes were selected at each cycle by binding to nitrocellulose filters, and the enriched RNAs were amplified by RT-PCR. Thirty cDNA clones, representing eight different sequences, were sequenced after round 5. Seven of the eight sequences share the pentanucleotide consensus element AGGGA/U, which occurs twice in two of the sequences (for which both alignments are shown). Additional partial matches also occur in several of the sequences but are not shown for simplicity. The same seven sequences also have a high G content (>50%), as indicated on the right.

purified a 60-kDa IPEB from calf thymus that behaved similarly to the mouse PYS-2 IPEB activity; i.e., it bound to the IPE and transactivated a reporter gene from the binding site in HeLa nuclear extracts. We also cloned a 420-bp cDNA by RT-PCR using partial amino acid sequence from the calf IPEB. The sequence of the product of this cDNA was highly homologous to those of the previously cloned human p54^{nrb} (10) and mouse NonO (38). In addition, all of the peptide sequences identified in the purified calf thymus IPEB were present within the p54^{nrb} and NonO sequences. Western analysis showed that a monoclonal antibody to the human p54^{nrb} reacted with the calf IPEB and PYS-2 IPEB and that the calf and PYS-2 IPEBs and p54^{nrb} had identical relative electrophoretic mobilities of 60 kDa. In vitro-transcribed and -translated p54^{nrb} bound to the IPE sequence, and p54^{nrb} expressed in HeLa cells transactivated a CAT reporter gene in an IPE-dependent manner. Furthermore, we localized the IPE-binding and transactivation domains of p54^{nrb} to the N and C termini, respectively. Thus, based on its sequence homology, molecular size, antibody cross-reactivity, DNA-binding specificity, and transcriptional activity, we established that p54^{nrb}/NonO is, like calf or PYS-2 IPEB, an IPE-binding transcription activator.

Although p54^{nrb} in HeLa cells functions as a transcription activator in vitro and in vivo, it did not do so in PYS-2 cells. In fact, endogenous p54^{nrb} activity was slightly reduced in cotransfection assays, suggesting the presence of a titratable factor in PYS-2 cells that interacts with p54^{nrb}. In F9 cells, p54^{nrb} failed to activate transcription in vitro and in vivo. Results from several experiments suggest that the transcriptional inactivity of p54^{nrb} in F9 cells is due to its inability to bind IPE. First, we showed by Western analysis that p54^{nrb} is present in F9 cells. Second, we showed by DNA affinity chromatography that F9 IPEB bound poorly to IPE, confirming our previous Southwestern data (23). Third, the GAL4(1–147)/C-terminus fusion protein was an effective transcription activator in F9 cells. Furthermore, we predict that the inability of F9 IPEB to bind IPE is due to absent or incomplete posttranslational modification, in view of the fact that the recombinant p54^{nrb} expressed in bacteria failed to bind IPE whereas p54^{nrb} translated in reticulocyte lysate, which contains mammalian kinases and other modification activities, bound to the IPE effectively.

In addition to being a transcription factor, p54^{nrb}, which contains two adjacent, canonical RRMs in its N terminus, is a single-stranded RNA-binding protein. We have shown here that recombinant p54^{nrb} binds with high affinity to short G-rich (≥50%) RNAs that contain one or more copies of the motif AGGGA/U compared to control RNAs of the same length that lack the motif. In the absence of other proteins, p54^{nrb} can bind to longer RNAs that lack precise copies of the motif, probably through a cooperative binding mode. For example, we showed binding of recombinant p54^{nrb} to β-globin pre-mRNA and mRNA, and previous work showed binding to the chicken β-tropomyosin first intron and to single-stranded ribohomopolymers, particularly poly(G) and poly(U) (17). Similarly, the splicing factor hnRNP A1, which also has two RRMs, binds cooperatively to most, if not all, cellular transcripts but has much higher affinity for short RNAs with the hexanucleotide motif UAGGGA/U (5), which, interestingly, comprises the pentanucleotide SELEX consensus for p54^{nrb}. Moreover, the oligonucleotides AGGGA, GGGU, GGGA, AGGG, and GGG are present at higher than expected frequencies in vertebrate introns (12, 28). In addition, p54^{nrb} appears to be a splicing factor. An affinity depletion experiment showed that depletion of p54^{nrb} inhibited splicing of β-globin in vitro (17). Mutational analysis revealed that the SELEX motif AGGGA/U is part of an intronic enhancer required for efficient splicing of chicken β-tropomyosin intron B7, which is known to cross-link to an unidentified protein very similar in size to p54^{nrb} (34). Thus, p54^{nrb} appears to be a splicing factor with limited but detectable nucleotide sequence and/or composition-based RNA-binding preferences. The same p54^{nrb} domain may be used for RNA and DNA binding; NonO was shown to bind RNA from the N terminus (38), while we showed that the same domain in p54^{nrb} binds to the IPE. Interestingly, however, the putative posttranslational modification appears to be required for DNA binding but not for RNA binding. This observation raises the interesting possibility that posttranslational modification serves to switch between RNA- and DNA-binding modes of the protein.

Besides having pre-mRNA-binding properties, p54^{nrb} has striking sequence similarity to the splicing factor PSF (10), which has been shown to be required for catalytic step II of splicing of an α-tropomyosin pre-mRNA in vitro (15). Human p54^{nrb} (471 amino acids) and human PSF (712 amino acids) are 70% identical in an internal ungapped region of 320 amino acids, the N-terminal half of which comprises both RRMs (10). In addition, p54^{nrb} and PSF are basic, and both proteins have proline- and glutamine-rich N termini (10, 30, 38) which are present not only in many transcription factors but also in many RNA-binding proteins (reference 30 and references therein). Thus, Patton et al. (30) hypothesized that the glutamine/proline- and proline-rich regions are binding sites for recognition and assembly of additional factors during the formation of transcription complexes and spliceosomes.

Given the extensive similarity between PSF and p54^{nrb}, it would be surprising if these two factors functioned in entirely different nuclear processes. Transcription and splicing are usu-

ally coupled in vivo, since many, though not all, introns are processed as part of nascent transcripts (reviewed in reference 35). An additional link between these two nuclear processes has been previously suggested, based on the observation that when in vivo splicing is reversibly inhibited by microinjection of oligonucleotides or antibodies that inhibit splicing, transcriptional activity is correspondingly reduced (29). Furthermore, the *Drosophila* B52 splicing factor was shown to cross-link in vivo to DNA that flanks the transcribed regions of the fully activated heat shock genes (6), suggesting association of B52 with the promoter. An ETS-related transcription factor, SPI-1/Pu.1, was recently shown to bind RNA, competing with p54^{nrb} binding, and to interfere with pre-mRNA splicing in vitro (13). Moreover, SPI-1/Pu.1 and p54^{nrb} appear to associate in vivo. Thus, transcription and RNA processing appear to be intimately connected nuclear processes that may share common factors (35, 37, 39). It will be of interest to determine the association of p54^{nrb} with promoter elements and transcribed regions of specific genes in vivo, which should further define its roles in nuclear processes.

ACKNOWLEDGMENTS

We thank G. Prendergast for critical reading of the manuscript, and we thank L. Showe and F. Rauscher III for helpful discussion.

This work was supported by Public Health Service grants GM37762 and GM47421 from the National Institute of General Medical Sciences (C.C.H.), by grants CA10815 from the National Cancer Institute and BIR-9318027 (to The Wistar Institute), and by grant CA13106 from the National Cancer Institute (A.R.K.).

REFERENCES

1. **Aebersold, R. H., J. Leavitt, R. A. Saavedra, L. E. Hood, and S. B. H. Kent.** 1987. Internal amino acid sequence analysis of proteins separated by one- or two-dimensional gel electrophoresis after in situ protease digestion on nitrocellulose. Proc. Natl. Acad. Sci. USA **84:**6970–6974.
2. **Ausubel, F. M., R. Brent, R. E. Kingston, D. D. Moore, J. G. Seidman, J. A. Smith, and K. Struhl (ed.).** 1990. Current protocols in molecular biology, p. 10.81–10.86. Green Publishing Associates and Wiley Interscience, John Wiley and Sons, New York, N.Y.
3. **Birney, E., S. Kumar, and A. R. Krainer.** 1993. Analysis of the RNA-recognition motif and RS and RGG domains: conservation in metazoan pre-mRNA splicing factors. Nucleic Acids Res. **21:**5803–5816.
4. **Burd, C. G., and G. Dreyfuss.** 1994. Conserved structures and diversity of functions of RNA binding proteins. Science **265:**615–621.
5. **Burd, C. G., and G. Dreyfuss.** 1994. RNA binding specificity of hnRNP A1: significance of hnRNP A1 high-affinity binding sites in pre-mRNA splicing. EMBO J. **13:**1197–1204.
6. **Champlin, D. T., and J. T. Lis.** 1994. Distribution of B52 within a chromosomal locus depends on the level of transcription. Mol. Biol. Cell **5:**71–79.
7. **Chang-Yeh, A., D. E. Mold, and R. C. C. Huang.** 1991. Identification of a novel murine IAP-promoted placenta-expressed gene. Nucleic Acids Res. **19:**3667–3672.
8. **Christy, R. J., and R. C. C. Huang.** 1988. Functional analysis of the long terminal repeats of intracisternal A-particle genes: sequences within the U3 region determine both the efficiency and direction of promoter activity. Mol. Cell. Biol. **8:**1093–1102.
9. **DeAngelo, D. J., J. Defalco, L. Rybacki, and G. Childs.** 1995. The embryonic enhancer-binding protein SSAP contains a novel DNA-binding domain which has homology to several RNA-binding proteins. Mol. Cell. Biol. **15:** 1254–1264.
10. **Dong, B., D. S. Horowitz, R. Kobayashi, and A. R. Krainer.** 1993. Purification and cDNA cloning of HeLa cell p54^{nrb}, a nuclear protein with two RNA recognition motifs and extensive homology to human splicing factor PSF and Drosophila NonA/Bj6. Nucleic Acids Res. **21:**4085–4092.
11. **Ellis, L., E. Clauser, D. O. Morgan, M. Edery, R. A. Roth, and W. J. Rutter.** 1986. Replacement of insulin receptor tyrosine residues 1162 and 1163 compromises insulin-stimulated kinase activity and uptake of 2-deoxyglucose. Cell **45:**721–732.
12. **Engelbrecht, J., S. Knudsen, and S. Brunak.** 1992. G+C-rich tract in 5′ end of human introns. J. Mol. Biol. **227:**108–113.
13. **Falzon, M., and E. L. Kuff.** 1989. Isolation and characterization of a protein fraction that binds to enhancer core sequences in intracisternal A-particle long terminal repeats. J. Biol. Chem. **264:**21915–21922.
14. **Falzon, M., and E. L. Kuff.** 1991. Binding of the transcription factor EBP-80 mediates the methylation response of an intracisternal A-particle long terminal repeat promoter. Mol. Cell. Biol. **11:**117–125.
15. **Gozani, O., J. G. Patton, and R. Reed.** 1994. A novel set of spliceosome-associated proteins and the essential splicing factor PSF bind stably to pre-mRNAa prior to catalytic step II of the splicing reaction. EMBO J. **13:**3356–3367.
16. **Hager, D. A., and R. R. Burgess.** 1980. Elution of proteins from sodium dodecyl sulfate-polyacrylamide gels, removal of sodium dodecyl sulfate, and renaturation of enzymatic activity: results with sigma subunit of Escherichia coli RNA polymerase, wheat germ DNA topoisomerase, and other enzymes. Anal. Biochem. **109:**76–86.
17. **Hallier, M., A. Tavitian, and F. Moreau-Gachelin.** 1996. The transcription factor Spi-1/PU.1 binds RNA and interferes with the RNA-binding protein p54^{nrb}. J. Biol. Chem. **271:**11171–11181.
18. **Howe, C. C., and G. C. Overton.** 1986. Expression of an intracisternal A particle is elevated during differentiation of embryonal carcinoma cells. Mol. Cell. Biol. **6:**150–157.
19. **Kamat, J. P., A. Basu, K. Satyamoorthy, L. Showe, and C. C. Howe.** 1995. IPEB transcription factor regulating the intracisternal A particle gene during F9 cell differentiation is expressed at sites of lymphoid development. Mol. Reprod. Dev. **41:**8–15.
20. **Krainer, A. R., T. Maniatis, B. Ruskin, and M. R. Green.** 1984. Normal and mutant human β-globin pre-mRNAs are accurately and efficiently spliced in vitro. Cell **36:**993–1005.
21. **Kuff, E. L.** 1990. Intracisternal particle in mouse neoplasia. Cancer Cells **2:**398–400.
22. **Kuff, E. L., and K. K. Lueders.** 1988. The intracisternal A particle gene family: structural and functional aspects. Adv. Cancer Res. **51:**183–276.
23. **Lamb, B. T., K. Satyamoorthy, L. Li, D. Solter, and C. C. Howe.** 1991. CpG methylation of an endogenous retroviral enhancer inhibits transcription factor binding and activity. Gene Expression **1:**185–196.
24. **Lamb, B. T., K. Satyamoorthy, D. Solter, A. Basu, M. Q. Xu, R. Weinmann, and C. C. Howe.** 1992. A DNA element that regulates expression of an endogenous retrovirus during F9 cell differentiation is E1A dependent. Mol. Cell. Biol. **12:**4824–4833.
25. **Leslie, K. B., F. Lee, and J. W. Schrader.** 1991. Intracisternal A-type particle-mediated activations of cytokine genes in a murine myelomonocytic leukemia: generation of functional cytokine mRNAs by retroviral splicing events. Mol. Cell. Biol. **11:**5562–5570.
26. **Lueders, K. K., J. W. Fewell, E. L. Kuff, and T. Koch.** 1984. The long terminal repeat of an endogenous intracisternal A-particle gene functions as a promoter when introduced into eukaryotic cells by transfection. Mol. Cell. Biol. **4:**2128–2135.
27. **Meitz, J. A., J. W. Fewell, and E. L. Kuff.** 1992. Selective activation of a discrete family of endogenous proviral elements in normal BALB/c lymphocytes. Mol. Cell. Biol. **12:**220–228.
28. **Nussinov, R.** 1989. Conserved signals around the 5′ splice sites in eukaryotic nuclear precursor mRNAs: G-runs the frequent in the introns and C- in the exons near both 5′ and 3′ splice sites. J. Biomol. Struct. Dyn. **6:**985–1000.
29. **O'Keefe, R. T., A. Mayeda, C. L. Sadowski, and A. R. Krainer.** 1994. Disruption of pre-mRNA splicing in vivo results in reorganization of splicing factors. J. Cell Biol. **124:**249–260.
30. **Patton, J. G., E. B. Porro, J. Galceran, P. Tempst, and B. Nadal-Ginard.** 1993. Cloning and characterization of PSF, a novel pre-mRNA splicing factor. Genes Dev. **7:**393–406.
31. **Sadowski, I., and M. Ptashne.** 1989. A vector expressing Gal4(1-147) fusion in mammalian cells. Nucleic Acids Res. **17:**7539.
32. **Satyamoorthy, K., K. Park, M. L. Atchison, and C. C. Howe.** 1993. The intracisternal A-particle upstream element interacts with transcription factor YY1 to activate transcription: pleiotropic effects of YY1 on distinct DNA promoter elements. Mol. Cell. Biol. **13:**6621–6628.
33. **Schindelin, H., M. A. Marahiel, and U. Heinemann.** 1993. Universal nucleic acid-binding domain revealed by crystal structure of the B. subtilis major cold-shock protein. Nature (London) **364:**164–168.
34. **Sirand-Pugnet, P., P. Durosay, E. Brody, and J. Marie.** 1995. An intronic (A/U)GGG repeat enhances the splicing of an alternative intron of the chicken beta-tropomyosin pre-mRNA. Nucleic Acids Res. **23:**3501–3507.
35. **Spector, D. L.** 1993. Macromolecular domains within the cell nucleus. Annu. Rev. Cell Biol. **9:**265–315.
36. **Tsai, D. E., D. S. Harper, and J. D. Keene.** 1991. U1-snRNP-A protein selects a ten nucleotide consensus sequence from a degenerate RNA pool presented in various structural contexts. Nucleic Acids Res. **19:**4931–4936.
37. **Xing, Y., C. V. Johnson, P. R. Dobner, and J. B. Lawrence.** 1993. Higher level organization of individual gene transcription and RNA splicing. Science **259:**1326–1330.
38. **Yang, Y-S., J. H. Hanke, L. Carayannopoulos, C. M. Craft, J. D. Capra, and P. W. Tucker.** 1993. NonO, a non-POU-domain-containing, octamer-binding protein, is the mammalian homolog of *Drosophila nonA^{diss}*. Mol. Cell. Biol. **13:**5593–5603.
39. **Zhang, G., K. L. Taneja, R. H. Singer, and M. R. Green.** 1994. Localization of pre-mRNA splicing in mammalian nuclei. Nature (London) **372:**809–812.
40. **Zierler, M., R. J. Christy, and R. C. C. Huang.** 1992. Nuclear protein binding to the 5′ enhancer region of the intracisternal A particle long terminal repeat. J. Biol. Chem. **267:**21200–21206.